Gradient-index fiber-optic microprobes for minimally invasive *in vivo* low-coherence interferometry

William A. Reed,* Man F. Yan,* and Mark J. Schnitzer

Bell Laboratories, Lucent Technologies, 600 Mountain Avenue, Murray Hill, New Jersey 07974

Received April 23, 2002

We describe the design, construction, and application of what are believed to be the smallest fiber-optic probes used to date during imaging or diagnosis involving low-coherence interferometry (LCI). The probes use novel fiber-optic gradient-index (GRIN) lenses fabricated by a recently developed modified chemical-vapor-deposition (MCVD) process that avoids on-axis aberrations commonly marring MCVD-fabricated GRIN substrate. Fusing GRIN fiber lenses onto single-mode fiber yields automatically aligned all-fiber probes that insert into tissue through hypodermic needles as small as 31-gauge (inner diameter, 127 μm). We demonstrate the use of such probes with LCI by measuring microscopic brain motions *in vivo*. © 2002 Optical Society of America

OCIS codes: 170.4580, 170.4500, 170.3340, 060.2370.

Unlike optical imaging within hollow tissues, invasive imaging within solid tissue generally leads to tissue damage from mechanical insertion of the optical probe. Tissue damage is a key issue not only for human patient care but also for work with small animals, in which entire anatomical nuclei may be <1 mm across. Existing optical probes often have diameters in the millimeter range, so it is critical to develop smaller invasive probes that are compatible with current imaging modalities.

Low-coherence interferometry (LCI) is the physical technique underlying important imaging modalities such as optical coherence tomography[1] and optical Doppler tomography.[2,3] LCI is usually implemented as a fiber interferometer and has been used to study surface tissues such as skin[4] or retina[5] and hollow tissues[6] such as respiratory or digestive tracts. A smaller set of invasive studies has also been performed.[7] LCI probes are commonly 0.4–3 mm in diameter, and the smallest probe reported uses a 27-gauge thin-walled hypodermic needle [inner diameter (i.d.), 0.3 mm; outer diameter (o.d.), 0.41 mm].[7] We report here fiber lens probes that can be delivered via hypodermics up to 31-gauge (i.d., 127 μm; o.d., 254 μm) but that preserve the optical advantages of LCI.

A key benefit of LCI is the ability to selectively acquire signals from a chosen depth within the sample by adjusting the optical path length of the interferometer reference arm. Axial resolution in LCI is determined by the coherence length, δ, of the optical source and is typically chosen as ~2–17 μm (e.g., Refs. 1 and 5). The number of axial sections that can be acquired without degrading lateral resolution by more than a factor of $\sqrt{2}$ is determined by $2z/\delta$, where the Rayleigh range, z, is typically ~200–950 μm for LCI (e.g., Refs. 5 and 6). A beam emitted from single mode-fiber (SMF) has $z \sim 25$–70 μm, so the beam must be collimated. LCI probes often employ gradient-index (GRIN) lenses, which do not rely on curved refractive surfaces and can be cheaply fabricated in submillimeter sizes. Yet the size of GRIN lenses used[6,7] (~250–600 μm diameter) has been a limiting factor. We overcame this by developing lenses based on GRIN fiber that are more than twice as small, ranging from 100 to 300 μm in diameter.

Glass GRIN lenses are conventionally fabricated by ion exchange, in which a cation is introduced into the glass in a spatially inhomogeneous manner to produce a refractive-index gradient.[8] We introduce the refractive-index gradient into GRIN fiber lenses using optical fiber production methods. Ge-doped GRIN preform was fabricated by use of modified chemical-vapor deposition (MCVD), in which glass layers of different refractive indices are sequentially introduced in a cylindrical glass tube.[9] The preform was pulled to create GRIN fiber with a nearly parabolic radial refractive-index profile (Fig. 1). As in conventional GRIN lenses, the waist of an optical beam will oscillate periodically as the beam travels along the fiber axis. Thus, short lengths (e.g., <2 mm) of this fiber can function as lenses. Previous efforts[10] to use pieces of MCVD-fabricated fiber for GRIN lenses commonly suffered from a refractive-index dip on the fiber axis that was an artifact of MCVD fabrication. This yielded lenses with on-axis aberrations. However, recent efforts to produce 10-Gbit/s ethernet fiber have led to MCVD techniques (e.g., Ref. 11) for producing GRIN preform nearly lacking the central index depression.

We used such improved preforms, which were originally designed to yield fiber with 125-μm o.d. and 50-μm-diameter GRIN core (OFS LaserWave).

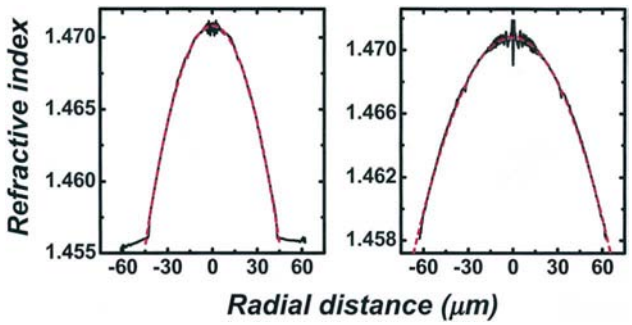

Fig. 1. Radial refractive-index profiles for two GRIN fiber lenses. Solid curves, index data as measured by the refracted near-field technique; red dashed curves, quadratic fits.

0146-9592/02/201794-03$15.00/0

Etching away some or all of the preform cladding with hydrofluoric acid before pulling to a final o.d. of 100–130 μm yielded a GRIN fiber core of 70–125 μm in diameter (e.g., Fig. 1). Varying the amount of material removed provided flexibility in our choice of the lens pitch, determined to first order by the quadratic coefficient in the refractive-index profile, $n(r) = n_0(1 - g^2r^2/2)$. The pitch, $p = 2\pi/g$, determines the length of fiber needed to make lenses with desired focal properties. We calculated these properties by use of the *ABCD* matrix formulation of Gaussian optics.[10]

Consider a beam of wavelength λ emitted from SMF with an initial beam waist w_0 through a GRIN fiber lens of length L (Fig. 2a). The beam then enters a medium of refractive index n'. The beam focus in the medium is located at a focal distance

$$f = \frac{n'\left(1 - \frac{\tilde{w}^4}{{w_0}^4}\right)\cos(gL)\sin(gL)}{gn_0\left[\sin^2(gL) + \frac{\tilde{w}^4}{{w_0}^4}\cos^2(gL)\right]}$$

from the lens face, where $\tilde{w}^2 = \lambda/(\pi g n_0)$ and the beam waist at f is

$$w = \frac{\lambda}{\pi n_0 w_0 g\left[\sin^2(gL) + \frac{\tilde{w}^4}{{w_0}^4}\cos^2(gL)\right]^{1/2}}.$$

This yields $z = n\pi w^2/\lambda$.

We fabricated a variety of GRIN fibers with g of 2–4 mm^{-1}. With these fibers, varying lens lengths spliced to Corning SMF-28 yield w values of up to ~33 μm and z values of up to ~2300 μm in air. By use of an integrated fusion splicer and cleaver (Vytran FFS-2000), 200–2000 μm of GRIN fiber could be fused to SMF and cleaved to form a lens on the SMF tip (Fig. 2a). The axial lens length was cleaved and measured to ~25- and 1-μm accuracy, respectively, with the aid of video microscopy and image analysis (Fig. 2b). For lenses with little or no cladding, splicing to SMF requires heating offset from the junction by ~50–100 μm so that glass viscosity mismatches during fusion are avoided. These procedures yielded lensed SMF probes that were automatically aligned.

To test design accuracy and possible effects of slight deviations from a parabolic refractive-index profile (Fig. 1), we measured the ability of SMF–GRIN probes to couple light back into another SMF. We used lenses of length about equal to the predicted $^1/_2$-pitch length and fused each end of the lenses to 10 m or more of SMF. We found that insertion loss was minimum when the lens length was within 1% of the predicted $^1/_2$-pitch length (Fig. 2c). The minimum loss of only ~0.05 dB or ~1% is within the range expected for a splice of SMF to SMF, indicating that the GRIN fiber lens refocuses the beam to nearly its original diameter. These observations show that the lens pitch and beam waist are within ~1% of predicted values, despite slight deviations from a purely quadratic index profile (Fig. 1).

GRIN fiber lenses form the basis for a variety of all-fiber optical probes for LCI and other applications. We fabricated compound fiber lenses that combine GRIN elements with different g values (Fig. 3a) or that combine GRIN elements with uniform quartz rod to yield an even wider range of collimation or focusing parameters. This capability is important for applications requiring high-N.A. focusing, because singlet GRIN fiber lenses cannot focus a beam to a tighter focus than the initial waist.

To facilitate insertion into tissue, probes are often delivered via hypodermic needles. Our 125-μm-diameter probes easily insert through a standard 30-gauge hypodermic (i.d., 152 μm; o.d., 300 μm), three gauges smaller than what are believed to be the tiniest needles used previously[7] with LCI. Our smallest probes combine an 80-μm-diameter SMF and a 100-μm-diameter GRIN fiber lens. These probes can be delivered via 31-gauge hypodermic (i.d., 127 μm; o.d., 254 μm; Fig. 3b). Some endoscopes for LCI employ a radial scanning configuration in which the beam emerges at an angle to the fiber axis and is rotated for scanning imaging in a manner akin to radar.[6,7] We fabricated GRIN fiber lens probes in which a piece of 125-μm-diameter uniform quartz fiber was fused to the tip of the lens and polished at an angle to permit a beam emitted at an angle to the

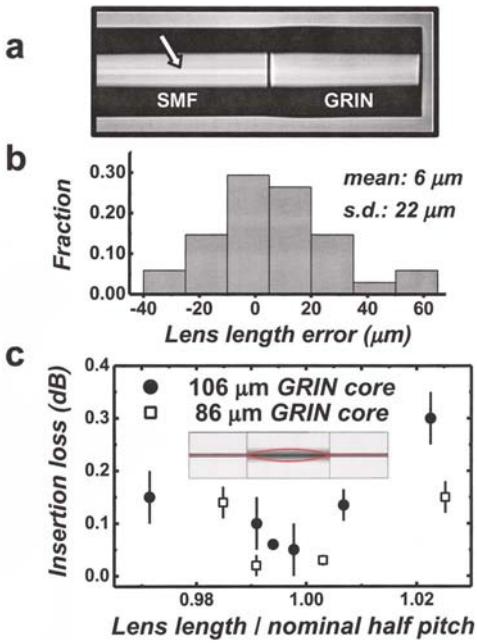

Fig. 2. a, GRIN fiber lens fused to SMF (125 μm). The image of SMF reveals a sharp boundary (arrow) between core and cladding, unlike the lens. b, Histogram of length differences between intended and actual lens lengths. c, Mean insertion loss on splicing a GRIN fiber lens of nearly $^1/_2$-pitch length into the middle of SMF for two different GRIN lens types. Lens lengths are normalized by predicted $^1/_2$-pitch length. Measurements were performed with 1.4–1.6 μm excitation by use of a stabilized light source and an optical spectrum analyzer. Loss varies systematically due to wavelength dependence in the $^1/_2$-pitch length. The bars are not error bars but indicate the full range of loss over 1.4–1.6 μm. Inset, schematic depicting lens, SMF, and beam expansion.

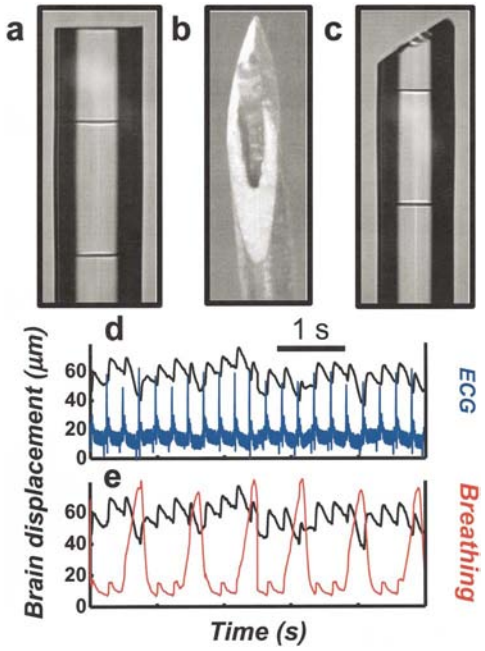

Fig. 3. a, Composite 125-μm-diameter probe with two GRIN lens elements fused to SMF. b, 80-μm-diameter SMF fused to a 100-μm-diameter GRIN fiber lens delivered via a 31-gauge needle (127-μm i.d., 254-μm o.d.). c, GRIN fiber lens probe for rotational scanning LCI, consisting of SMF fused to a GRIN fiber lens and a coreless quartz fiber. The quartz is angled so that the beam is emitted off axis and traces a cone when the fiber is rotated. d, e, Brain motion measured by LCI with a Ti:sapphire laser source compared to cardiac and respiratory signals. Black traces, brain displacement. d, Blue trace, electrocardiogram. e, Red trace, chest displacement measured with a piezoelectric sensor.

fiber axis (Fig. 3c). These probes can be mechanically rotated and optically coupled with established approaches.[7]

To demonstrate the use of our probes in combination with LCI, we performed invasive *in vivo* measurements of brain motion in anesthetized rats. Such motion often represents a major problem for *in vivo* brain studies, because it can disrupt the mechanical stability of physiological probes such as electrodes and thereby terminate physiological recordings. Voluntary movements, as well as cardiac and respiratory pulsations, can cause brain motions of $\sim$50 μm even after skull immobilization.[12] It was recently shown that interferometric methods can be used to measure brain motion, permitting real-time motion compensation in the position of a physiological probe.[12] Here we use GRIN fiber lens probes and LCI to monitor brain motions *in vivo*.

We performed a craniotomy above the somatosensory cortex of rats anesthetized with urethane. A bare GRIN fiber lens probe with focal length $<$350 μm was inserted $\sim$300 μm into the cortex perpendicular to the brain surface. Respiratory rate was monitored with a piezoelectric sensor on the chest, and cardiac activity was monitored by electrocardiogram. We used LCI in a manner akin to optical Doppler tomography[2,3] to measure brain motion at fixed locations as far as $\sim$400 μm from the probe tip with $\lesssim$1-kHz bandwidth. Interferometric brain displacement traces reveal pulsations of up to $\sim$40 μm (Figs. 3d and 3e). These motions seem largely cardiac related, since they appear in sync with the $\sim$5-Hz heartbeat. Between heartbeats, brain tissue position relaxes nearly monotonically at $\sim$40–150 μm/s. Such measurements should be useful for keeping an additional, e.g., electrophysiological, probe stationary relative to the brain[12] (M. J. Schnitzer and M. S. Fee, to be published).

We have applied recent advances in ethernet fiber fabrication toward all-fiber probes for use with minimally invasive LCI. These probes involved fiber lenses that are essentially free from on-axis index aberrations, are over three times as small as previously described LCI probes, and to our knowledge are the smallest lensed probes to date for *in vivo* tissue studies. Other applications of our lenses may involve fiber-coupled optical sources, micro-optical switches, or beam-expanded fiber.

We thank D. Mazzarese and X. Jiang for providing preform and the Bell Labs draw team for making fiber. We enjoyed conversations with A. Yablon, F. Helmchen, W. Denk, B. Bouma, and J. Izatt. Our brain motion studies are an ongoing collaboration between M. S. Fee and M. J. Schnitzer. Animal procedures performed in accordance with NIH guidelines. Scientific correspondence should be sent to schnitzer@lucent.com; requests for materials, to mfy@ofsoptics.com.

*Present address, Optical Fiber Solutions, Murray Hill, New Jersey 07974.

References

1. D. Huang, E. A. Swanson, C. P. Lin, J. S. Schuman, W. G. Stinson, W. Chang, M. R. Hee, T. Flotte, K. Gregory, C. A. Puliafito, and J. G. Fujimoto, Science **254,** 1178 (1991).
2. Y. Zhao, Z. Chen, Z. Ding, H. Ren, and J. S. Nelson, Opt. Lett. **27,** 98 (2002).
3. V. Westphal, S. Yazdanfar, A. M. Rollins, and J. A. Izatt, Opt. Lett. **27,** 34 (2002).
4. B. H. Park, C. Saxer, S. M. Srinivas, J. S. Nelson, and J. de Boer, J. Biomed. Opt. **6,** (2001).
5. W. Drexler, U. Morgner, R. K. Ghanta, F. X. Kärtner, S. Schuman, and J. G. Fujimoto, Nat. Med. (N.Y.) **7,** 502 (2001).
6. G. J. Tearney, M. E. Brezinski, B. E. Bouma, S. A. Boppart, C. Pitris, J. F. Southern, and J. G. Fujimoto, Science **276,** 2037 (1997).
7. X. Li, C. Chudoba, C. Ko, C. Pritris, and J. Fujimoto, Opt. Lett. **25,** 1520 (2000).
8. B. Messerschmidt, U. Possner, and S. N. Houde-Walter, Appl. Opt. **36,** 8145 (1997).
9. J. B. MacChesney, Proc. IEEE **68,** 1181 (1980).
10. W. L. Emkey and C. A. Jack, J. Lightwave Technol. **5,** 1156 (1987).
11. J. C. Rousseau and R. Sauvageon, "Method of controlling the etching and collapse of an MCVD tube by monitoring internal pressure," U.S. patent 6,131,413 (October 17, 2000).
12. M. S. Fee, Neuron **27,** 461 (2000).